

https://doi.org/10.1070/QEL16847

Conversion of light polarisation in asymmetric plasmonic waveguides

I.A. Pshenichnyuk, S.S. Kosolobov, A.I. Maimistov, V.P. Drachev

Abstract. **Hybrid plasmonic waveguides with an embedded conducting oxide layer can be used for producing fast and compact electro-optical modulation devices. However, due to constraints, which plasmon modes impose on light polarisation, modulators of this class are not compatible with high-efficiency modern diffraction gratings used for coupling light into a waveguide. In the present work we demonstrate how a simple structuring of a modulation sandwich makes it possible to produce a compact polarisation converter that eliminates the mentioned incompatibility.**

Keywords: *plasmonic waveguide, transparent conducting oxide, electro-optical modulator, polarisation converter, surface plasmon polariton.*

1. Introduction

Characteristic dimensions of computers have quickly decreased for several decades, whereas their performance has grown. Modern transistors of size ~10 nm can operate at frequencies of several gigahertz. Prospect for their further miniaturisation face a number of challenges, the main one being a transfer from nano- to molecular electronics [1, 2]. Nevertheless, the weak point of modern calculation systems is not a transistor dimension or efficiency but communication between various electronic units [3]. We mean the connection not only between autonomous schematic elements such as a central processor, memory unit, and graphical processor, but between elements inside chips, for example, between cash and processor cores. A conventional solution to the connection problem, well demonstrated at long distances (from one computer to another) is the employment of light. Integration of the elements of classical photonics to nanoelectronics and their employment at short distances is limited by a light wavelength and the diffraction limit, which prevents compression of a light signal to nanometre-scale dimensions. It is possible to eliminate the dimension discrepancy problem and provide fast connection at short distances due to technologies of sub-wavelength optics and new materials [3]

A key element in nanophotonics is an electro-optical modulator, that is, a device that modulates an optical signal by electric one. According to the above discussion, the modulator should be small, fast and consume a minimal energy. A promising candidate may be the plasmonic modulator described in [4]. Compactness of the device is attained due to the employment of hybrid plasmonic waveguides [5] by transforming part of the optical signal to a subwave plasmonic mode. To this end, dielectric and metal layers are evaporated onto a conventional silicon waveguide. For signal modulation, a thin layer of transparent conducting oxide ITO is imbedded into a sandwich. The real part of a layer dielectric function can turn to zero at a certain concentration of charge carriers [6]. By using an external field for producing a domain with an increased electron concentration in ITO one can obtain a well-pronounced modulation effect.

A weak feature of such a modulator is limitation on the modulated signal polarisation. In a hybrid waveguide, a plasmon mode can only be excited by the light polarised normally to the metal–dielectric interface. Since the layers of the modulation sandwich are evaporated horizontally, the modulator only operates with vertically polarised light. The most convenient method to introduce light into a waveguide is the employment of grating couplers. Presently, the best results (with an input efficiency of ~100%) are obtained for horizontally polarised light [7]. In the present work we demonstrate how a compact polarisation rotator can be made by performing elementary lithographic structuring of the sandwich. In this case, the order of layers and material compositions remain unchanged providing maximal compatibility. The employment of such a device along with a plasmonic modulator can solve the polarisation problem.

2. Theory

Here we present calculations, which demonstrate operation of a plasmonic modulator and polarisation converter. In the modelling, the frequency-domain Maxwell equations are solved numerically:

$$\nabla \times \boldsymbol{E} = +\mathrm{i}\omega\mu\boldsymbol{H}, \tag{1}$$

$$\nabla \times \boldsymbol{H} = -\mathrm{i}\omega\varepsilon\boldsymbol{E}, \tag{2}$$

where $\boldsymbol{E}$ and $\boldsymbol{H}$ are the vectors of electric and magnetic field strengths; ω is the light frequency; and μ and ε are the magnetic permeability (assumed equal to unity) and dielectric

I.A. Pshenichnyuk, S.S. Kosolobov Skolkovo Institute of Science and Technology, ul. Nobelya 3, 121205 Moscow, Russia;
e-mail: i.pshenichnyuk@skoltech.ru;
A.I. Maimistov National Research Nuclear University 'MEPhI', Kashirskoe sh. 31, 115409 Moscow, Russia;
V.P. Drachev Skolkovo Institute of Science and Technology, ul. Nobelya 3, 121205 Moscow, Russia; present address: University of North Texas, USA, 76203 Texas, Denton, 1155 Union Circle

Received 9 October 2018
Kvantovaya Elektronika **48** (12) 1153–1156 (2018)
Translated by N.A. Raspopov

function of a medium. Obviously, the latter is a function of coordinates and frequency, that is, $\varepsilon = \varepsilon(x,y,z,\omega)$ and is unique for each of the materials employed.

A model dielectric function for conducting materials (in our case these are gold, doped silica, and ITO) is given by the Drude formula:

$$\varepsilon(\omega) = \varepsilon_\infty - \frac{\omega_p^2}{\omega^2+\gamma^2} + i\frac{\gamma\omega_p^2}{\omega(\omega^2+\gamma^2)}, \quad (3)$$

where ε_∞ is the asymptotic value of the dielectric function at high frequencies; γ is the damping factor, which is a function of the charge carrier mobility; and ω_p is the plasma frequency. The latter depends on the charge density n_c, electron charge e and its effective mass m^*:

$$\omega_p = \sqrt{\frac{n_c e^2}{\varepsilon_0 m^*}}. \quad (4)$$

One can easily see that the real part of the dielectric function turns to zero at the following electron concentration

$$n_{enz} = \frac{m^*}{e^2}\varepsilon_\infty\varepsilon_0(\omega^2+\gamma^2). \quad (5)$$

In such a material as ITO, at a light wavelength $\lambda = 1550$ nm the dielectric function turns to zero at the electron concentration $n_{enz} = 6.5\times10^{20}$ cm^{-3}. In view of the fact that the initial level of ITO doping may be within the range of 10^{19}–10^{21} cm^{-3} [8], the epsilon-near-zero effect is applicable for switching the modulator state.

Equations (1) and (2) are solved numerically in 3D-space. The models were constructed by using large non-uniform meshes, which, as a consequence, requires a large RAM (~400 Gb). The calculations presented in this work were performed in a Pardus cluster (Skoltech, Moscow). The modelling employed a commercial software Comsol Multiphysics with an additional module Wave Optics. Required material parameters were taken from the Material Library module and literature [9, 10].

3. Calculation results and discussion

A cross-section view of a plasmonic modulator is shown in Fig. 1a. The cross section and complete 3D model of a polarisation converter is shown in Figs 1b and 1c, respectively. In both devices, a sandwich comprised of the ITO (10 nm), SiO_2 (20 nm), and Au (200 nm) layers is deposited onto a silicon waveguide with the cross section 400 × 400 nm. The difference is that in the polarisation rotator the sandwich covers half the waveguide only (Fig. 1b). In our calculations, the sandwich longitudinal size varied from 5 to 15 μm. A modulation UHF signal is applied to a gold contact of the electro-optical modulator. Operation of the rotator implies zero voltage, and gold plays the role of a plasmonic material only, which forms a hybrid waveguide (although, the case of a non-zero voltage at the rotator contact is considered below for completeness). The similar layer sequences and thicknesses in the modulator and rotator is an important constructive feature, which provides high compatibility of both the devices and simple fabrication, which reduces to lithographic structuring of evaporated layers. In the present paper, according to Fig. 1, under the light

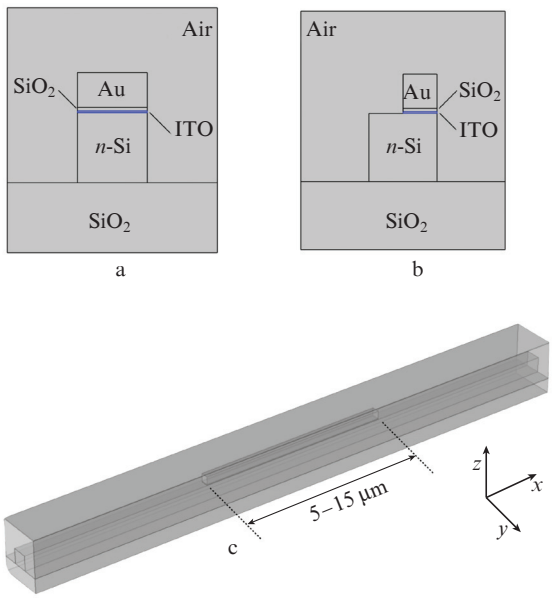

Figure 1. Geometry of modelled devices: (a) cross section of the plasmonic modulator, (b) cross section of the polarisation converter, and (c) 3D-model of the polarisation converter.

horizontal polarisation we imply the direction parallel to the plane on which the waveguide is arranged and perpendicular to the waveguide itself (y axis). The direction normal to both the plane and the waveguide (z axis) corresponds to the vertical polarisation.

Results of 3D modelling for light passage through the modulator are shown in Fig. 2, where the square electric field in the vertical cross section of the device is plotted. In the on-state of the modulator, the gold contact voltage is zero. Since the initial doping level of ITO in our calculations is 10^{20} cm^{-3}, the material mainly behaves as a dielectric

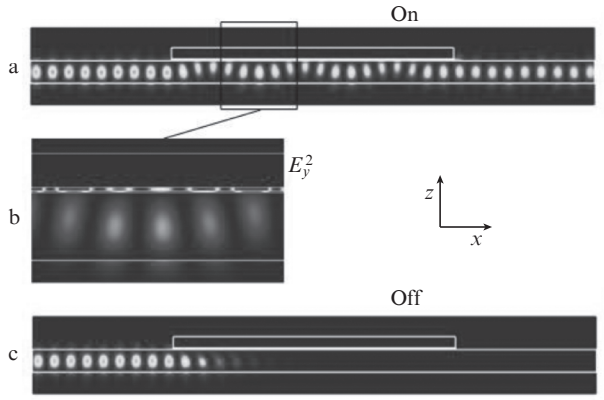

Figure 2. Results of modelling of light propagation through the plasmonic modulator in (a) on-state and (c) off-state. The concentrations of charge carriers in the active ITO layer are 10^{20} and 7.5×10^{20} cm^{-3}, respectively (the maximal resonance in a thin ITO layer slightly shifts relative to its volume value obtained in Sect. 2). Light is vertically polarised (along z axis normally to the modulation sandwich). Optical losses with the switched on modulator are 24%. A close-up view in Fig. 2b presents the field distribution for the plasmonic mode in a sandwich (the modulator is switched on).

exhibiting negligible conducting properties. In this case, the waveguide mode passing into the modulator is converted to a hybrid plasmonic mode and then it is converted back at the output. Here, attenuation is related to optical losses only, which are 24%. Since hybrid modes are generated in pairs, there are beats in the domain where the modulation sandwich acts. In this example, light is vertically polarised. A horizontally polarised signal passes through the modulator actually without changes.

As the voltage is applied, an electric field begins to act on the ITO layer, which results in the formation of a layer enriched with charges. As the critical concentration n_{enz} is reached, the ITO dielectric function turns to zero. The device geometry is such that the active layer resides in the domain where the plasmonic mode intensity is maximal, and the layer efficiently interacts with the passing light. The continuity requirement for the normal projection of the electric induction vector at the ITO–dielectric interface results in that the field intensity inside the ITO layer substantially increases. Since the imaginary part of the dielectric function also substantially increases at a higher electron concentration in the active layer, the ITO layer efficiently suppresses the 'trapped' field. The field distribution in the case of a voltage applied to the gold contact is shown in Fig. 2c. Here, the optical losses are almost 100%, and the modulator is in off-state. A close-up view in Fig. 2b gives the field distribution in the plasmonic mode for the switched on modulator (with the maximal transmission). One can see that in the hybrid mode, the field maximum is in the plasmonic component.

Results of modelling the light passage through the polarisation converter are presented in Fig. 3. The input waveguide mode in this example is horizontally polarised (in contrast to the previous example), which corresponds to the light launched through a diffraction grating [7]. A horizontal field projection is shown in Figs 3a and 3c, and arising vertical projection is presented in Figs 3b and 3d. Similarly to the case of the modulator, the vertical cross section of the device is shown. A field picture without a voltage applied to the gold contact is given in Figs 3a and 3b; one can see that the vertical projection needed for modulation arises, disappears, and arises again at the rotator output. The device length, which in this case equals to 15 μm, is sufficient to contain 1.5 beat periods. Obviously, with such an oscillation character of mode conversion, the device length will directly affect the conversion efficiency. In the rotator shown in Fig. 3, about 50% of the intensity of the mode with the initial horizontal polarisation is converted to a vertically polarised mode. These are direct analogues of the processes occurring in directional couplers [11]. Analysis of the mode conversion is complicated by the fact that the theory of coupled waves well developed for directional couplers, is not adequate in the case of hybrid plasmonic waveguides [5]. This is explained by strong interaction between plasmonic and waveguide modes and, as a consequence, lacking small parameter for constructing approximations. The development of such a theory is an important task for future work. Qualitatively, an asymmetric modulation sandwich (which just covers part of the width of the waveguide) provides coupling between the modes with horizontal and vertical polarisations, which do not interact otherwise. The indirect interaction of modes results in oscillations shown in Fig. 3. In [12], this effect is

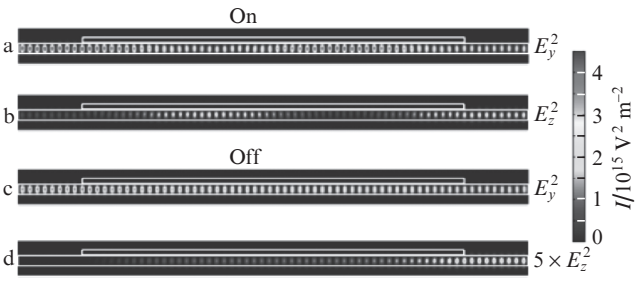

Figure 3. Field distribution in the polarisation rotator in cases (a, b) without voltage at the gold contact and (c, d) with the voltage applied (similarly to the modulator, the latter case is marked 'off', which corresponds to a suppressed optical signal). (a, c) Horizontal y-component and (b, d) vertical z-component of the field are shown. Signal in Fig. 3d is amplified by a factor of 5 for better visualisation.

described in the mode analysis language and for other plasmonic materials.

When the voltage is applied, the mode conversion picture changes (Figs 3c and 3d) so that only 20% of the initial signal intensity is converted to the vertical mode (for better view, the field z-component in Fig. 3d is increased by a factor of 5). First of all, this is related to activation of the ITO layer, which begins to absorb the converted mode. The active layer also influences the character of mode coupling, which affects the length of beats (seemingly, it becomes much longer than the device length). The dependence of the polarisation converter behaviour on the contact voltage gives a chance to combine the modulator and rotator into a single device capable of operating with a radiation of arbitrary polarisation. However, in the geometry considered the characteristics of such a modulator (in particular, the extinction coefficient) are sufficiently modest. For this reason, at the present stage it is more appropriate to speak about two separate devices: a polarisation rotator and an electro-optical modulator, which are similar in the sandwich structure but have different geometries. The development of a plasmonic modulator operating with arbitrarily polarised radiations ocan be a task for future work in this direction.

Finally, note that the present work suggests a simple solution of the polarisation problem for plasmonic modulators. The model of the polarisation converter suggested is similar to the modulator itself, which simplifies its practical realisation. Numerically demanding 3D calculations have been performed, which confirmed the concept suggested and gave its quantitative estimate.

Acknowledgements. This work was supported by the Ministry of Education and Science of the Russian Federation (Project No. RFMEFI58117X0026).

References

1. Pshenichnyuk I.A., Cizek M. *Phys. Rev. B*, **83**, 165446 (2011).
2. Pshenichnyuk I.A., Coto P.B., Leitherer S., Thoss M. *J. Phys. Chem. Lett.*, **4**, 809 (2013).
3. Liu K., Ye C.R., Khan S., Sorger V.J. *Laser Photon. Rev.*, **9**, 172 (2015).
4. Sorger V.J., Lanzillotti-Kimura N.D., Ma R.M., Zhang X. *Nanophotonics*, **1**, 17 (2012).

5. Alam M.Z., Aitchison J.S., Mojahedi M. *Laser Photon. Rev*., **8**, 394 (2014).
6. Alam M.Z., De Leon I., Boyd R.W. *Science*, **352**, 795 (2016).
7. Michaels A., Yablonovich E. *Opt. Express*, **26**, 4766 (2018).
8. Kulkarni A.K., Knickerbocker S.A. *J. Vac. Sci. Technol*., **14**, 1709 (1996).
9. Melikyan A., Lindenmann N., Walheim S., Leufke P.M., Ulrich S., Ye J., Freude W. *Opt. Express*, **19**, 8855 (2011).
10. Sinatkas G., Pitilakis A., Zografopoulos D.C., Beccherelli R., Kriezis E.E. *J. Appl. Phys*., **121**, 023109 (2017).
11. Harris N.C. PhD Thesis (MIT, USA, 2017).
12. Kim S., Qi M. *Opt. Express*, **23**, 9968 (2015).